Bifurcation of gap solitons through catastrophe theory

C. Conti and S. Trillo
Department of Engineering, University of Ferrara, Via Saragat 1, 44100 Ferrara, Italy
and Istituto Nazionale di Fisica della Materia (INFM)-RM3, Via della Vasca Navale 84, 00146 Roma, Italy
(Received 10 April 2001; published 30 August 2001)

In the theory of optical gap solitons, slowly-moving finite-amplitude Lorentzian solutions are found to mediate the transition from bright to coexistent dark-antidark solitary wave pairs when the laser frequency is detuned out of the proper edge of a dynamical photonic band gap. Catastrophe theory is applied to give a geometrical description of this strongly asymmetrical ''morphing'' process.

DOI: 10.1103/PhysRevE.64.036617 PACS number(s): 42.65.Tg

The confinement of optical radiation in periodic media (gratings) with nonlinear response occurs in the form of gap solitons (GS), or more properly solitary waves, as first predicted by Chen and Mills [1], and studied extensively afterwards [2–8]. In Kerr media, the prototype model for GS is the following system of hyperbolic partial differential equations with Hamiltonian (conservative) structure [9,10], which couples the forward $u_+(z,t)$ and backward $u_-(z,t)$ propagating envelopes at Bragg carrier frequency ω_B

$$\begin{aligned} i(\partial_t+\partial_z)u_+ + u_- + (X|u_-|^2+S|u_+|^2)u_+ = 0, \\ i(\partial_t-\partial_z)u_- + u_+ + (X|u_+|^2+S|u_-|^2)u_- = 0. \end{aligned} \tag{1}$$

Equations (1) have been conveniently written in usual dimensionless units $z=\Gamma Z$ and $t=\Gamma V_B T$, where Z and T are the real-world propagation distance and time, Γ is the Bragg coupling coefficient, and V_B is the group velocity at Bragg frequency. Moreover S and X are coefficients that specify the relative weight of self- and cross-phase modulation, and $u_\pm$ are proportional to real-world envelope amplitudes. Equations (1) are usually analyzed with $S=1$ and $X=2$ (one of the two coefficients can be always set to have unitary modulus by a suitable rescaling of the field amplitudes) that describes *scalar*-mode coupling, e.g., in optical fiber gratings [2–6]. Conversely we find convenient to leave them as generic coefficients in order to describe both the cases of focusing ($S,X>0$ [2–5]) and defocusing ($S,X<0$ [1]) nonlinearity, as well as the two limit cases $X=0$ and $S=0$, which arise, e.g., when the cubic nonlinearity originates from cascading in quadratic media [11,12]. Cascading adds improved flexibility since it permits to control the sign of the effective Kerr nonlinearity by tuning the wave-vector mismatch. We also emphasize that, in the case $S=0$, Eqs. (1) reduce to the integrable (by means of the inverse scattering method) massive Thirring model, and hence the localized waves are strictly speaking solitons.

Despite the fact that GS arise in a variety of physical settings and models, the importance of Eqs. (1) is threefold.

(i) They describe with reasonable accuracy optical GS experimentally investigated in fiber Bragg gratings [7] and in corrugated GaAs waveguides [8].

(ii) Though not integrable by inverse scattering method (except for the massive Thirring case), the model allows to construct the whole family of solitary waves.

(iii) Equations (1) have allowed to assess the occurrence of peculiar effects such as the onset of oscillatory instabilities [9,10], ultimately related with the absence of material dispersion (i.e., second-order derivatives) which distinguishes Eqs. (1) from other soliton-bearing dispersive models (e.g., those of the nonlinear Schrödinger type).

GS of Eqs. (1) have been studied for more than a decade, and both bright [2,3] and dark [4] solutions were reported. Yet, the existence of such GS solutions and their bifurcations (how they change qualitatively against changes of parameters) were never investigated to full extent. Here we unveil the bifurcation structure of GS, restricting ourselves to subluminal solutions for physical reasons. We show that moving Lorenztian GS mark the transition between in-gap bright GS and dark-antidark GS pairs that coexist either below or above (depending on the focusing or defocusing nature of the nonlinearity, respectively) the edge of a suitably defined dynamical gap. We also link this dynamical gap to the stop band usually defined in the stationary coupled-mode theory of Bragg gratings, discussing why the former is more important and why, in our opinion, the distinction between *gap* and *Bragg* bright solitons seems artificial.

Following the notation of Ref. [10], the entire family of solitary waves of Eqs. (1) can be characterized by seeking solutions in the form

$$\begin{aligned} u_+(z,t) = U_+\sqrt{\eta(\zeta)}\exp\{-i\Delta t + i[\beta\zeta+\phi_+(\zeta)]\} \\ u_-(z,t) = U_-\sqrt{\eta(\zeta)}\exp\{-i\Delta t + i[\beta\zeta+\phi_-(\zeta)]\}, \end{aligned} \tag{2}$$

where $\beta\equiv\gamma v\Delta$ plays the role of GS propagation constant, and the intensity η and the chirp (nonlinear phase) $\phi_\pm$ profiles depend on $\zeta\equiv\gamma(z-vt)$, with $\gamma=(1-v^2)^{-1/2}$ being the (subluminal, $|v|<1$) Lorentz factor. Furthermore $U_+ = A\sqrt[4]{(1+v)/(1-v)}$ and $U_- = -sA\sqrt[4]{(1-v)/(1+v)}$ account for the velocity-induced asymmetry between the foward and backward modes, whereas $s\equiv\mathrm{sgn}[X(1-v^2)+S(1+v^2)]$ is the sign of the nonlinearity that appears only through

the common overall coefficient $A=\gamma^{-1}|2X(1-v^2)+2S(1+v^2)|^{-1/2}$. Importantly the entire family of GS is characterized by two independent parameters [so-called *internal* parameters to be distinguished by the *external* parameters X and S that appear in Eqs. (1)], namely, the normalized detuning Δ and soliton velocity v. These correspond, in real-world units, to $\delta\omega=\Gamma V_B\Delta$ and $V=V_B v$, and are related to rotational and translational group symmetries of Eqs. (1), respectively [10]. Note that $\Delta=0$ corresponds to the Bragg frequency, and $v=0$ yields still GS, i.e., confinement of light with zero velocity in the lab frame.

By direct substitution of Eqs. (2) into Eqs. (1), it is readily verified that the intensity η and overall phase $\theta\equiv\phi_+-\phi_-$ obey the following one-dimensional (thus integrable) Hamiltonian system of equations

$$\dot{\eta}=2\eta\sin\theta=-\frac{\partial H}{\partial\theta},$$
$$\dot{\theta}=2\delta+2\cos\theta-\eta=\frac{\partial H}{\partial\eta}, \tag{3}$$

where the dot stands for $d/d\zeta$, $H=H(\eta,\theta)=2\eta\cos\theta+2\delta\eta-\eta^2/2$ is the reduced-conserved ($\dot{H}=0$) Hamiltonian, which now depends on the single parameter $\delta\equiv\gamma\Delta$. In Eqs. (1) and hereafter we implicitly assume to deal with the self-defocusing nonlinearity $s=-1$ originally considered in Ref. [1], including the case of vanishing S or X. The results can be readily extended to the self-focusing case $s=1$ with the substitution $\theta\to2\pi-\theta$ and $\delta\to-\delta$. Importantly, the latter condition means that the role of frequencies below and above Bragg frequency must be simply interchanged.

The reduced system (3) permits to find the solitary waves of Eqs. (1) as the separatrix trajectories that are homoclinic to (i.e., emanate from and return to) the unstable fixed points η_s,θ_s of Eqs. (3). Given the constraint $\eta>0$ in Eq. (2), these are easily found to be of two kinds: (i) $(\eta_s,\cos\theta_s)=(0,-\delta)$ for $\delta^2<1$, which is associated with solutions of the bright type since $\eta(\zeta=\pm\infty)=\eta_s=0$; (ii) $(\eta_s,\theta_s)=[2(\delta-1),\pi]$ for $\delta>1$, which describe GS with nonvanishing background or pedestal $\eta(\zeta=\pm\infty)=\eta_s=2(\delta-1)$. For any fixed value of the parameter δ, the solitary waves correspond, in both cases, to level curves of the Hamiltonian $H_s=H(\eta_s,\theta_s)$.

Let us first clarify the relation between the existence domain of these two families of GS and the stop band or forbidden gap of frequencies exhibited by the grating in the linear operation regime. Bright solutions exist for $|\delta|<1$, which is mapped into the inner domain $\Delta^2+v^2<1$ of the parameter plane Δ,v (such representation was already adopted in Refs. [10,13]). This unitary circle can be regarded as a *dynamical gap*, since in this domain the linear problem [i.e., Eqs. (1) with $S,X=0$] yields exponentially damped traveling-wave solutions [$u^{\pm}\propto\exp(-i\Delta t+iQ\zeta)$, with $Q^2<0$]. On the other hand, solutions with nonzero pedestal exist only outside this dynamical gap or unitary circle.

To clarify further the role of the soliton velocity v, it is important to link the dynamical gap $\Delta^2+v^2<1$ with the band gap (henceforth termed *rest gap* to rule out any possible source of misunderstanding) of the stationary linear coupled-mode problem. Such rest gap is well known to be related to the reflectivity bandwidth of the grating, in turn measurable by means of a tunable cw laser in the laboratory (or rest) frame (z,t). Quantitatively, the rest gap is given by the frequency range $|\delta_1|<1$ ($|\delta\omega_1|<\Gamma V_B$ in real-world units) where solutions $u_\pm(z,t)=u_\pm(z)\exp(-i\delta_1 t)$ with frequency detuning δ_1 (real-world frequency $\omega_B+\delta\omega_1$) are exponentially damped in space, at variance with the out-gap case $|\delta_1|>1$ where they become oscillatory [14]. In the velocity-frequency plane (v,δ_1) the rest gap is the (v-independent) lighter-shaded domain shown in Fig. 1(a), which has a clear one-to-one correspondence with the reflectivity bandwidth reported for comparison in Fig. 1(b). To map the dynamical band gap in the same parameter plane, we need to know what is the actual normalized GS frequency detuning in the rest frame, which is readily found to be $\delta_1\equiv\gamma^2\Delta$ by grouping in Eqs. (2) phase terms proportional to t. In other words the excitation of a GS characterized by the parameters v and Δ requires a source with detuning $\delta_1=\gamma^2\Delta$ from Bragg frequency. As a consequence the dynamical gap where bright GS exist, can be mapped onto the whole shaded domain $\delta_1^2<\gamma^4(1-v^2)$ or equivalently $|\delta_1|<\gamma$ of Fig. 1. It is clear that, for any given velocity v, this entails a frequency range that is wider than the rest gap $|\delta_1|<1$ and reduces to it only in the $v=0$ limit. As a consequence bright GS exist for frequencies ranging from the rest gap (reflectivity bandwidth) in the $v=0$ case, to the whole frequency axis as $|v|\to1$ (i.e., as the soliton velocity V approaches the linear group velocity V_B in the forward or backward direction).

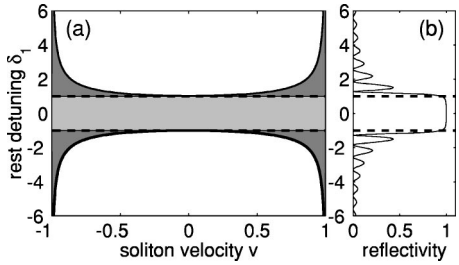

FIG. 1. (a) The dynamical photonic band gap (whole shaded domain) $|\delta_1|<\gamma$ in the parameter plane of velocity and rest detuning (v,δ_1). Such domain is mapped back onto the inner domain bounded by the circle $\Delta^2+v^2=1$ in the plane (Δ,v), see Fig. 2. The rest band gap $|\delta_1|<1$ is the smaller region between the two dashed lines $\delta_1=\pm1$ (light shaded area), and corresponds to the bandwidth of the linear reflectivity curve shown with the same vertical scale in (b) for a grating of normalized length $z_L=\Gamma L=4$.

As far as the terminology is concerned, a last important comment is in order. Bright solitary solutions of Eqs. (1) are usually classified as gap solitons or Bragg solitons, depending on their detuning δ_1 being inside ($|\delta_1|<1$, light-shaded domain in Fig. 1) or outside ($1<|\delta_1|<\gamma$, dark-shaded domain in Fig. 1) the rest gap, respectively. Though such a distinction can be useful to locate the operating frequency with respect to the reflectivity bandwidth of the grating, it appears otherwise rather artificial. First, for any given velocity v there are no qualitative changes of the solutions by

crossing the boundary $|\delta_1|=1$ between these two regions. Second, and more important, the picture of Fig. 1 suggests that all the existing bright-localized waves are in fact *gap* solitons if referred to the dynamical gap. In other words, the plot of Fig. 1(a) can be interpreted by saying that the effective frequency gap seen by a soliton that moves at velocity v is wider (the faster the soliton the wider the gap) than the rest gap measured through the reflectivity in the rest frame. This is also supported by the fact that δ can be interpreted as the frequency detuning of the soliton in Lorentz transformed variables ζ,τ with $\tau=\gamma(t-vz)$ [15]. Therefore the rest gap condition $|\delta_1|<1$ must be replaced in moving soliton coordinates by the condition $|\delta|=|\delta_1|/\gamma<1$ that coincides with the dynamical gap.

As far as the excitation of bright GS is concerned, one should correctly refer to the dynamical (wider) gap as the proper region of existence. In general one can achieve control on the input laser frequency detuning (i.e., δ_1) and the beam profiles, but not on the velocity. When $|\delta_1|>1$, so that the laser operates outside the rest gap (as it is usually the case in experiments carried out in fiber gratings), it is immediately clear from Fig. 1(a) that one has a lower bound $v_{low}^2=1-\delta_1^{-2}$ on the square velocity of the excitable solitons. In other words only solitons that travel with velocity $|v|>v_{low}=(1-\delta_1^{-2})^{1/2}$ (in both directions) do exist and can be excited. In the limit of infinite-frequency detunings ($|\delta_1|\to\infty$) from Bragg frequency, $v_{low}\to 1$, and solitons can only travel at linear group velocity. Conversely, inside the rest gap ($|\delta_1|<1$), such limitation does not hold, and solitons with any velocity $|v|<1$ can be excited. Ideally, a particular value of velocity is selected by matching the input beam profile (intensity and phase) to the solution that corresponds to that particular value of velocity. However, this can be hardly done in practice because, even assuming that there is no change of frequency in the process of soliton formation, the actual field profile inside the grating is affected by strong reflection at the grating boundary, and the velocity, in general, cannot be predicted with simple arguments. Moreover, one should consider that the excitation of a soliton requires, besides existence, also to fulfill the requisite of stability [9,10]. Incidentally, the decay of an unstable GS can be accompanied by changes of both internal parameters, frequency and velocity.

In order to find the GS profiles consider that Eqs. (3) are equivalent to the motion of an ideal particle of unitary mass and total energy E in a quartic potential well $U(\eta)$, ruled by the equation $\ddot{\eta}=-\partial U/\partial\eta$. The kinetic energy is easily obtained in the standard form from the first of Eqs. (3) by eliminating $\sin\theta$ through H, which yields

$$\dot{\eta}=\sqrt{2[E-U(\eta)]}, \tag{4}$$

where $U=-2\delta H\eta-\frac{1}{2}(4-4\delta^2-H)\eta^2-\delta\eta^3+\frac{1}{8}\eta^4$, and $E=-H^2/2$. The GS solutions can be worked out explicitly by inverting the quadrature integral obtained from Eq. (4) with the energy $E=-H_s^2/2$ pertaining to the unstable fixed point. For the case (i) $|\delta|<1$, we found expressions for the intensity $\eta(\zeta)$ and phase $\theta(\zeta)$ [explicit expressions for the phases $\phi_{\pm}(\zeta)$ can be also found], which entail GS of the bright type

$$\eta_B=\frac{4(1-\delta^2)}{\cosh(2\sqrt{1-\delta^2}\zeta)-\delta}, \tag{5}$$

$$\theta_B=\tan^{-1}\left[\frac{\sqrt{1-\delta^2}\sinh(2\sqrt{1-\delta^2}\zeta)}{-1+\delta\cosh(2\sqrt{1-\delta^2}\zeta)}\right]. \tag{6}$$

Close to the low-frequency edge of the dynamical gap $\delta\sim-1$, the following approximation of the intensity profile in Eq. (5) holds valid [exploit $\cosh(2x)=2\cosh^2(x)-1$ and $1-\delta^2\sim 2(1+\delta)$]

$$\eta_B=4(1+\delta)\,\mathrm{sech}^2(\sqrt{2(1+\delta)}\zeta), \tag{7}$$

which is characteristic of the one-soliton solution of the focusing nonlinear Schrödinger equation, which is known to provide a reasonable description of GS in this region of the gap [5,16].

In the case (ii), i.e. for $\delta>1$ two solutions coexist, being associated with two branches of a double-loop separatrix. The first one represents a dark soliton

$$\eta_{DK}=2(\delta-1)\frac{\cosh(2\sqrt{\delta-1}\zeta)-\sqrt{\delta}}{\sqrt{\delta}\cosh(2\sqrt{\delta-1}\zeta)+1}, \tag{8}$$

$$\theta_{DK}=\tan^{-1}\left[\frac{4\sqrt{\delta-1}(\delta+1)\sinh(2\sqrt{\delta-1}\zeta)}{3\delta^2+2\delta^{3/2}-3+4(\delta-1)\delta\cosh(2\sqrt{\delta-1}\zeta)+(\delta^2-2\delta^{3/2}-1)\cosh(4\sqrt{\delta-1}\zeta)}\right], \tag{9}$$

whereas the second one is a bright on pedestal or so-called antidark solution [17]

$$\eta_{AK}=2(\delta-1)\frac{\sqrt{\delta}\cosh(2\sqrt{\delta-1}\zeta)+1}{\sqrt{\delta}\cosh(2\sqrt{\delta-1}\zeta)-1}, \tag{10}$$

$$\theta_{AK}=\tan^{-1}\left[\frac{4\sqrt{\delta-1}\sqrt{\delta}\sinh(2\sqrt{\delta-1}\zeta)}{2-3\delta+\delta\cosh(4\sqrt{\delta-1}\zeta)}\right]. \tag{11}$$

These dark and antidark solutions specialized to the zero-velocity case ($v=0$) have important implications in terms of

the stationary ($\partial_t=0$) response of the grating, inducing limiting or frustrated bistability, as discussed in Ref. [18].

Right on the high-frequency edge of the dynamical gap, i.e., for $\delta\to 1$, the dark GS vanishes ($\eta_{DK}\to 0$), while the bright and the antidark solutions have the following common limit:

$$\eta_{LZ}=\frac{8}{1+(2\zeta)^2}, \tag{12}$$

$$\theta_{LZ}=\tan^{-1}\left[\frac{4\zeta}{(2\zeta)^2-1}\right], \tag{13}$$

which represents a finite-amplitude moving Lorentzian soliton, i.e., a GS with Lorentzian intensity profile. The existence of an exact solution of Eqs. (1) with nonexponentially decaying tails can be understood from the dynamical system (3) as being associated with a degenerate fixed point at the origin with zero eigenvalues. The fact that the Lorentzian shape approximates well bright GS close to the upper bound of the gap was noticed earlier under strictly stationary conditions ($v=0$) [6].

Vice versa, for $\delta\to -1$, i.e., close to the low-frequency edge of the dynamical gap, the intensity of the bright GS in Eq. (5) [or, consistently, of its nonlinear Schrödinger approximation (7)] reduces to the following Lorentzian profile

$$\eta_{LZ}=\frac{4(1+\delta)}{1+4\dfrac{1+\delta}{1-\delta}\zeta^2}\cong\frac{4(1+\delta)}{1+2(1+\delta)\zeta^2}. \tag{14}$$

In this case, however, as the stop-band edge is approached the Lorentzian GS (14) becomes broader and smaller, and eventually vanishes identically ($\eta_B\to 0$) for $\delta=-1$. The difference between the finite-amplitude [Eq. (13)] and the vanishing-amplitude [Eq. (14)] Lorentzian GS accounts for an intrinsic asymmetry of the nonlinear grating operation with respect to interchange of frequencies below and above the Bragg frequency, respectively.

Figure 2 summarizes the nature of the different GS solutions by reporting the intensity profiles $|u_\pm|^2$ of qualitatively different GS solutions sampled in the parameter plane (Δ,v). First, it must be noticed that still ($v=0$) GS have equal intensities $|u_+|^2=|u_-|^2$ as a consequence of the fact that the net photon flux is zero, for both in-gap (bright) and out-gap (dark-antidark) solutions. Moreover, let us recall that the amplitude of the in-gap (bright) GS increases and their width decreases by spanning the gap from left to right. The symmetry $|u_+|^2=|u_-|^2$ is broken for moving GS, which have a stronger component in the direction of motion (i.e., $|u_+|>|u_-|$ for $v>0$ and $|u_-|>|u_+|$ for $v<0$). Importantly, bright GS that have high amplitude (see HA inset in Fig. 2) close to the upper edge of the dynamical gap, become Lorentzian GS (LZ inset in Fig. 2) over the edge $\Delta+v^2=1$, and then bifurcate into dark-antidark pairs (DK and AK insets in Fig. 2) outside the dynamical bandgap. It is worth noting that the bright GS solutions with finite energy (or mass) bifurcate into this pair of solutions that, in an ideal infinite grating, have infinite energy due to their nonzero background. In a finite grating the excitation of such dark or antidark GS solutions is likely to be more critical than their bright counterpart, requiring proper excitation at the grating boundaries.

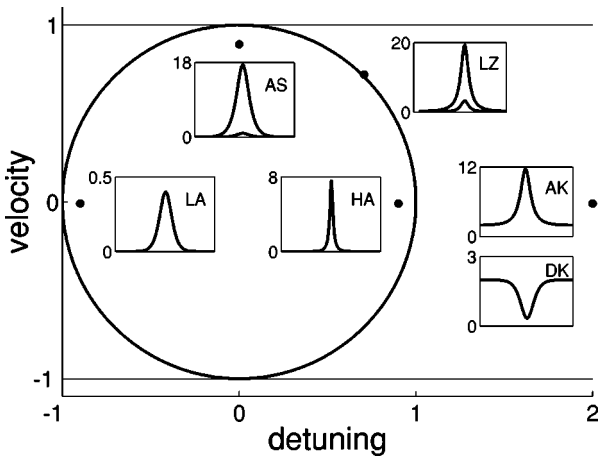

FIG. 2. Existence diagram (defocusing case) for subluminal GS in the region of detuning-velocity (Δ,v) plane bounded by the thin lines at $v=\pm 1$. The insets show GS intensity profiles $|u_\pm|^2$ sampled at the nearest marker (filled circle). Bright GS of low-amplitude (LA), high-amplitude (HA), and asymmetric (AS) types exist inside the dynamical gap (unitary circle $\Delta^2+v^2=1$). HA solitons become finite-amplitude Lorentzian (LZ) over the right semicircle, and then bifurcate into dark (DK) and antidark (AK) pairs, which coexist for frequencies above the upper edge of the dynamical bandgap. In the focusing case the same picture holds with $\Delta\to-\Delta$.

Vice versa, as explained above, the low-amplitude (LA inset) bright GS that exist close to the lower edge of the gap vanishes in the limit $\delta\to -1$, and no solutions exist below the bottom of the stop band (i.e., outside the circle for $\Delta<0$). For a focusing nonlinearity ($s=1$) an identical picture with $\Delta\to-\Delta$ holds true, meaning that the dark-antidark pairs originate always from the high-amplitude bright GS, though, in this case, they now exist below the low-frequency edge of the dynamical gap.

The bifurcation of GS can be effectively explained in terms of the catastrophe theory [19], and the underlying classification of the singularities of smooth functions. The quartic potential $U(\eta)$ belongs to the so-called cusp A_{+3} family [19]. It can be recast in the following standard form by means of the change of variable $\eta=\sqrt[4]{2}x+2\delta$, thus obtaining

$$\hat{U}(x)=\frac{1}{4}x^4+\frac{a}{2}x^2+bx, \tag{15}$$

where $a\equiv\sqrt{2}(-4-2\delta^2+H)$ and $b\equiv-8\sqrt[4]{2}\delta$. A necessary condition for the solitary waves to exist is that the potential $\hat{U}(x)$ has three critical points (i.e., such that $\partial\hat{U}/\partial x=0$), thus being of a double-well type. In the parameter plane (a,b) this occurs in a domain bounded by the following curve, so-called ''bifurcation set'' [19],

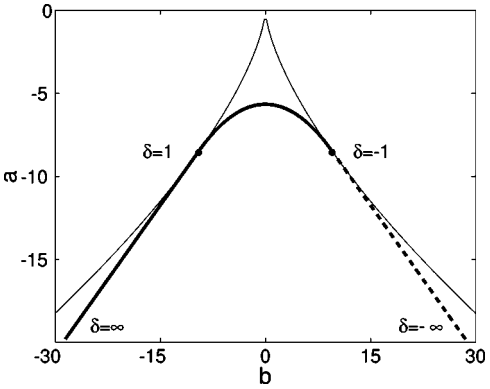

FIG. 3. Plot of the bifurcation set (thin line) from Eq. (16) and the control line (thick line) that gives the parametric dependence of the coefficients a and b of the potential $\hat{U}(x)$ in Eq. (15) on the control parameter δ, when this is varied from large-negative values ($\delta=-\infty$) to large-positive values ($\delta=\infty$). The dashed portion of the control line corresponds to unphysical solutions ($\eta<0$). Two catastrophes occur at the points $\delta=\pm 1$.

$$\left(\frac{a}{3}\right)^3+\left(\frac{b}{2}\right)^2=0, \tag{16}$$

which is reported as a thin-solid line in Fig. 3. As shown, this curve has the characteristic shape of a cusp. In the spirit of the catastrophe theory, we also report in Fig. 3 the so-called control line, i.e., how the parameters (a,b), and as a consequence the potential $\hat{U}$, vary by changing the single control parameter δ from large-negative values to large-positive values (indicated in Fig. 3 by the limit $\delta=-\infty$ and $\delta=\infty$, respectively). In doing so we calculate a with $H=H_s$, i.e., the value of the Hamiltonian pertaining to the solitons.

According to our analysis, by varying δ in the range $(-\infty,\infty)$ the control line remains always inside the cusp, indicating the possibility to have solitary waves. Dramatic qualitative changes of the solutions must be expected at the catastrophe points $\delta=\pm 1$ where the control line becomes tangent to the bifurcation set. In spite of the apparent symmetry of Fig. 3, the two catastrophes are the signature of the strongly asymmetrical behavior of GS against interchange of frequencies below ($\delta<0$) and above ($\delta>0$) the Bragg frequency. Indeed, the $\delta=1$ catastrophe marks the point where the maximum of the potential (15) moves from a finite positive value for $\delta>1$ (which makes accessible two distinct asymptotic evolutions inside the two wells, in turn corresponding to the dark and antidark GS), to the origin for $-1<\delta<1$ (where only one well is accessible for the asymptotic motion towards the origin that describes the bright GS). Conversely, the other catastrophe at $\delta=-1$ marks the point where these bright GS simply cease to exist because the maximum of the potential moves towards negative values. In fact, though the potential still has a double-well shape even for $-\infty<\delta<-1$, the possibility to have solitary waves is ruled out by the fact that the two wells become accessible only with $\eta<0$, and hence the solutions are unphysical (recall that η is an intensity). The dashed line in Fig. 3 displays that portion of the control line where the solutions are unphysical.

In summary we have shown that GS solutions of a well-known standard coupled-mode model with Kerr or Kerr-equivalent nonlinearity undergo a bifurcation that is strongly asymmetrical with respect to the Bragg frequency. The qualitative change of the solutions is explained with a geometrical picture based on the application of the catastrophe theory. The bifurcation is marked by the existence of finite-amplitude Lorentzian GS. In this sense it is reminiscent of the recently investigated case of localized waves sustained by a gap of full nonlinear origin [20]. In spite of the diversity between the bifurcation discussed here and that of Ref. [20], this suggests that Lorentzian solitons can play a universal role in the localization of light in periodic media.

We thank Yuri Kivshar for fruitful discussions concerning Lorentzian solitons.

[1] W. Chen and D.L. Mills, Phys. Rev. Lett. **58**, 160 (1987).
[2] A.B. Aceves and S. Wabnitz, Phys. Lett. A **141**, 37 (1989).
[3] D.N. Christodoulides and R.I. Joseph, Phys. Rev. Lett. **62**, 1746 (1989).
[4] J. Feng and F.K. Kneubül, IEEE J. Quantum Electron. **QE-29**, 590 (1993).
[5] C.M. De Sterke and J.E. Sipe, in *Progress in Optics XXXIII*, edited by E. Wolf (Elsevier, Amsterdam, 1994), Chap. III.
[6] D.L. Mills, *Nonlinear Optics* (Springer, New York, 1998).
[7] B.J. Eggleton, R.E. Slusher, C.M. de Sterke, P.A. Krug, and J.E. Sipe, Phys. Rev. Lett. **76**, 1627 (1996); B.J. Eggleton, C.M. de Sterke, and R.E. Slusher, J. Opt. Soc. Am. B **14**, 2980 (1997).
[8] P. Millar, R.M. De La Rue, T.F. Krauss, J.S. Aitchison, N.G.R. Broderick, and D.J. Richardson, Opt. Lett. **24**, 685 (1999).
[9] I.V. Barashenkov, D.E. Pelinovsky, and E.V. Zemlyanaya, Phys. Rev. Lett. **80**, 5117 (1998).
[10] A. De Rossi, C. Conti, and S. Trillo, Phys. Rev. Lett. **81**, 85 (1998); Opt. Lett. **23**, 1265 (1998).
[11] S. Trillo, Opt. Lett. **21**, 1732 (1996).
[12] C. Conti, G. Assanto, and S. Trillo, Opt. Lett. **22**, 1350 (1997).
[13] T. Peschel, U. Peschel, F. Lederer, and B.A. Malomed, Phys. Rev. E **55**, 4730 (1997).
[14] A. Yariv, *Optical Electronics in Modern Telecommunications* (Oxford University Press, New York, 1997).
[15] The Lorentz transformed time is written with light velocity $c=1$, consistently with the normalization of Eqs. (1). Let us point out that Eqs. (1) are not Lorentz invariant except in the integrable case $S=0$ of the massive Thirring model. However, the consequence that, in general, moving GS cannot be generated by means of a Lorentz transformation of the rest GS does not prevent us from using Lorentz transformed variables (see also Ref. [9]).
[16] C.M. de Sterke and B.J. Eggleton, Phys. Rev. E **59**, 1267

(1999); C.M. de Sterke, D.G. Salinas, and J.E. Sipe, J. Opt. Soc. Am. B **16**, 587 (1999).
[17] Y.S. Kivshar and V.V. Afanasjev, Phys. Rev. A **44**, R1446 (1991).
[18] S. Trillo, C. Conti, G. Assanto, and A.V. Buryak, Chaos **10**, 590 (2000).
[19] R. Gilmore, *Catastrophe Theory for Scientists and Engineers* (Dover, New York, 1993).
[20] C. Conti, S. Trillo, and G. Assanto, Phys. Rev. Lett. **85**, 2502 (2000).